Accepted manuscript (author version)

To appear in:

Iranian Journal of Earth Sciences (Iran J. Earth. Sci.)

E-ISSN: 2228-785X **Print ISSN:** 2008-8779

This PDF file is not the final version of the record. This version will undergo further copyediting, typesetting, and production review before being published in its definitive form. We are sharing this version to provide early access to the article. Please be aware that errors that could impact the content may be identified during the production process, and all legal disclaimers applicable to the journal remain valid.

Received: 3 December 2024

Revised: 12 January 2025

Accepted: 9 March 2025

DOI: https://doi.org/10.57647/j.ijes.2025.17555

Original Research

The effect of lithology and tectonic on the landslide occurrence and hazard zonation in the Dalanpar mountains, Zagros orogenic belt

Bahman Rahimzadeh[1*], Somaiyeh Khaleghi[2], Shahram Bahrami[2]

[1] Department of Mineral & Groundwater Resources, Faculty of Earth Sciences, Shahid Beheshti University, Tehran, Iran.

[2] Department of Physical Geography, Faculty of Earth Sciences, Shahid Beheshti University, Tehran, Iran

*Corresponding author: b_rahimzadeh@sbu.ac.ir

Abstract

The Dalanpar Mountains, located in the northwestern part of the Zagros Mountains, are highly active in terms of orogeny and morphology. Various types of landslides, such as successive landslides, rock falls, earth flows, and debris flows occur in this region. To assess the occurrence of landslides in this area, a combination of field geology and satellite imagery was utilized to identify landslides and perform susceptibility analysis based on the density area and the Landslide Numerical Risk Factor (LNRF) methods. Landslide hazard zonation maps indicate that the majority of landslides in the Dalanpar Mountains are in the high and very high hazard classes, and that geology, slope, slope aspect, precipitation, and land use factors have played significant roles in landslide occurrence. The high percentage of area under the success rate curves (AUC) for density area (72%) and LNRF (68%) methods demonstrates that both methods have accurately predicted the landslide susceptibility zonation map of the study area. Field observations indicate that lithological and structural factors are significant contributors to slope instability. Both field observations and landslide susceptibility analysis show that serpentinization plays a crucial role in slope instability, with most landslides occurring on serpentinite units. Reverse and strike-slip faults have significantly impacted the occurrence of landslides and increased the serpentinization process. Field observations reveal that large landslides have resulted in planar surfaces and depressions, where water has accumulated in some cases, creating seasonal and permanent lakes. The high activity rate and persistence of activity in the Dalanpar landslides indicate that, in addition to the usual factors affecting landslides such as slope and precipitation, they are strongly influenced

by the behavior of the serpentinite units and fault effects in the diapirism system with the positive flower structure in the dextral strike-slip fault mechanism.

Keywords: Serpentinization, Landslide, Hazard zonation, Active tectonics, Dalanpar Mountains, Zagros

1. Introduction

Landslides, as one of the most significant mass movements, are widespread in mountainous regions, especially in areas with active tectonics. Tectonic and lithological factors are commonly considered the most critical parameters influencing the occurrence and distribution of landslides (Roering et al. 2015; Conforti and Ietto, 2020). Tectonic features, such as faults, joints, and foliations, contribute to the fatigue of rock complexes and identify zones of weakness that may influence the size and shape of landslides (Carlini et al., 2016; Cirillo et al., 2024). Cui et al. (2018) proposed that geological structures, including joint sets, local faults, and folds, have affected the occurrence of the Daguangbao landslide on the northwestern limb of the Dashuizha Anticline in China.

Landslides that are influenced by lithological effects, particularly ophiolite mélange units, are also present along the Zagros orogeny and the Alpine-Himalayan belt in countries such as Turkey, Cyprus, Greece, and Italy (Christaras, 1997; Göncüoglu et al., 2014; Kojima et al., 2015; Carlini et al., 2016; Bahrami et al., 2020). In regions with abundant serpentinites, landslides frequently occur due to the high sliding potential of these rocks. While landslides in the Dalanpar Mountains are similar to those in other ophiolitic mélange areas, the impact of serpentinite units in the region and their relationship with landslides, as well as the formation of small and large lakes in the highlands, are still debated.

According to Bahrami et al. (2020), the occurrence of landslides in the Sarv-Abad region in Kurdistan, Iran, is strongly influenced by the combined effects of tectonic activity and lithology. They found that most landslides are located near major faults, including the Main Recent Fault (MRF) and the Main Zagros Reverse Fault (MZRF), where lithological units of marls and serpentinites, which have high potential for flexibility, lubrication, plasticity, and expansion, also play a significant role in landsliding. The effects of lithology and tectonic features in the occurrence and intensification of landslides are well documented by numerous studies (Zhang et al., 2016; Gaidzik et al., 2020; Delgado et al., 2022; Zhao et al., 2022; Machay et al., 2023). In addition to geology (lithology, faults, structural and geotechnical characteristics, etc.), other controlling factors of landslide occurrence include earthquakes, geomorphology (slope morphology, river incision, drainage network, weathering, subsidence, and deposition), climate (rainfall, snowmelt), topography (slope angle, slope aspect), and human activities (land use change, road construction, mining, etc.) (Bahrami et al., 2020).

The Zagros orogeny in Iran, which is part of the Alpine-Himalayan orogeny (Fig. S1), is considered one of the world's most tectonically active regions (Stocklin, 1968). The northern part of the Zagros orogeny exhibits a triple junction of the Arabian, Iranian, and Anatolian plates, which occurs at the border of Iran, Iraq, and Turkey (Karaoğlu et al., 2020) (Fig. 2a). The convergence of these three plateaus in the Paleogene (Rahimzadeh et al., 2019; Agard et al., 2001) led to the obduction of Oshnaviyeh ophiolites and the formation of the Dalanpar Mountains with an elevation of 3500 m above sea level. Landslides and various lakes have formed in these mountains, which are similar to the phenomena observed only in Sarvabad in the Zagros (Bahrami et al., 2020). Although large landslides have occurred in other parts of the Zagros (Shoaei, 2014; Ghazipour, 2015), there are significant differences in terms of formation and occurrence between this region and the South Zagros. Landslides are typically found in confluence zones such as unstable lithology and active tectonics (Huang et al., 2013), although the most notable examples of such events in the Zagros are seen in Seymareh (Kabirkuh).

Owing to the lithological characteristics, where marl layers exhibit similar rheology to serpentinite, one of the largest landslides in the world, Seimareh, occurred about ten thousand years ago in Kabirkuh, Zagros, with a length of approximately 11 km (Harrison and Falcon, 1937; Shoaei and Ghayoumian, 1998; Shoaei, 2014). In Sarvabad, numerous landslides have been caused by the combined effect of tectonics and serpentinite layers (Bahrami et al., 2020). Similarly, landslides have also been observed in the southern Zagros, Lorestan, and Bakhtiari regions, with a mechanism akin to Kabirkuh, which is attributed to the absorption of water by marls (Ghazipour, 2015).

In this research, we aim to investigate the reason for the high elevation of the serpentinites, which is an unusual case in Dalanpar (3550 m). This is important because serpentinites are among the most erodible and unstable rocks on the Earth's surface, yet they maintain a considerable elevation in Dalanpar.

High elevation persisting over geological time in unstable lithologies such as serpentinite can cause landslides in successive generations. It would be expected that, despite the occurrence of landslides and various erosive factors such as precipitation, there would eventually be a decrease in height and slope, leading to a reduction in landslide occurrence. The relationship between orogenic processes and the continuity of landslides in serpentine-dominated landscapes with active tectonics represents a novel perspective in this research that can explain the occurrence of multigenerational and continuous landslides.

We focused on studying landslides in this region for two main reasons:

1-Along the Zagros Mountain range, there are many mountains with similar heights and rainfall and steeper slopes than Dalanpar. For example, the Shahidan Mountains in the north with granite and schist composition and the Qandil Mountains in the south of the area are composed of limestone. However, no landslides have occurred in these areas. Conversely, in the Dalanpar Mountains, many landslides have occurred in different stages from the past to the present. Therefore, in addition to examining conventional factors such as precipitation, topographic slope, and land use, the effect of rock type and tectonic units was specifically investigated.

2-Despite many landslides from the past to the present that have continuously reduced the height and slope of the mountain, this mountain still has a similar height to the surrounding mountains, which likely indicates a different underlying tectonic force. To investigate this phenomenon, the geodynamics of the Dalanpar ophiolites and their orogenic mechanism were explored through field studies examining cross-sections in an east-west direction.

2. Materials and methods

2.1. Geology of Dalanpar area

The Zagros Belt features four prominent ophiolitic complexes, namely the Neyriz, Kermanshah, Kurdistan, and Khoy ophiolites, from south to north (Saccani et al., 2014). The Dalanpar ophiolites, which formed during the Paleocene period and were obducted in the late Oligocene (Pirouz et al., 2017), are situated between the Kurdistan and Khoy ophiolites in the northwestern region of the Zagros orogeny (Hajmolla Ali et al., 2005). During the compression of the Arabian plateau against the Iranian one, these ophiolites, together with associated sedimentary assemblages such as pelagic limestone and shale, gave rise to the Dalanpar and Bozsina mountains that reach elevations of approximately 3500 m a.s.l. The ophiolitic complexes in this region are widely exposed and encompass nearly all units of a complete ophiolite sequence of the Neo-Tethyan type (Dilek and Furnes, 2014). The ophiolite units consist of dismembered serpentinite, different types of gabbro, basalts, and ophiolite mélange assemblages, along with pelagic limestone sediments and radiolarite cherts that have undergone transformation in some regions. The calcareous-radiolarite units mainly constitute the sedimentary assemblage in higher horizons and mountain ridges (Hajmolla Ali et al., 2005). The ophiolite complex is bordered to the east by the Sanandaj-Sirjan phyllite/slate metamorphism and to the west by the high Zagros zone limestone.

The research site is situated at the junction of three plateaus, namely Arabian, Iranian, and Turkish, and encompasses the Main Zagros Thrust Fault (MZTF) and the Main Recent Fault (MRF). The area is characterized by frequent thrust and reverse faults associated with the confluence, which constitute the primary structural features. Ophiolitic complex units are closely associated with faults and are often controlled by MZTF and MRF (Tchalenko and Braud, 1974). Thus, the relationship between these units is predominantly through fault ophiolites, in which the order of the ophiolite assemblages has been lost and is now referred to as a mélange. The Bozsina and Espībenār overthrusts are the most significant thrust faults in the study region (Fig. 1b). The Main Recent Fault, characterized by a dextral slip mechanism and a north-northwest-southeast trend (330-300° north), exhibits significant activity in the region, cutting through numerous pre-existing structures (Mohajjel and Rasouli, 2014). The MRF of Zagros is comprised of several segments in Iran, including the Serow fault, which is situated within the study area and leads to the Piranshahr fault from the south (Fig. 1a) (Tchalenko and Braud, 1974). While lithology and tectonic factors individually can cause geomorphological phenomena like landslides and lake formation, their combined impact is even more pronounced. For instance, in areas where the young Zagros fault intersects with the region and active tectonics are present, multiple generations of numerous phenomena have taken place among the four ophiolite assemblages in the Zagros. One noteworthy example is the Sarvabad ophiolites, which have experienced widespread landslides (Bahrami et al., 2020).

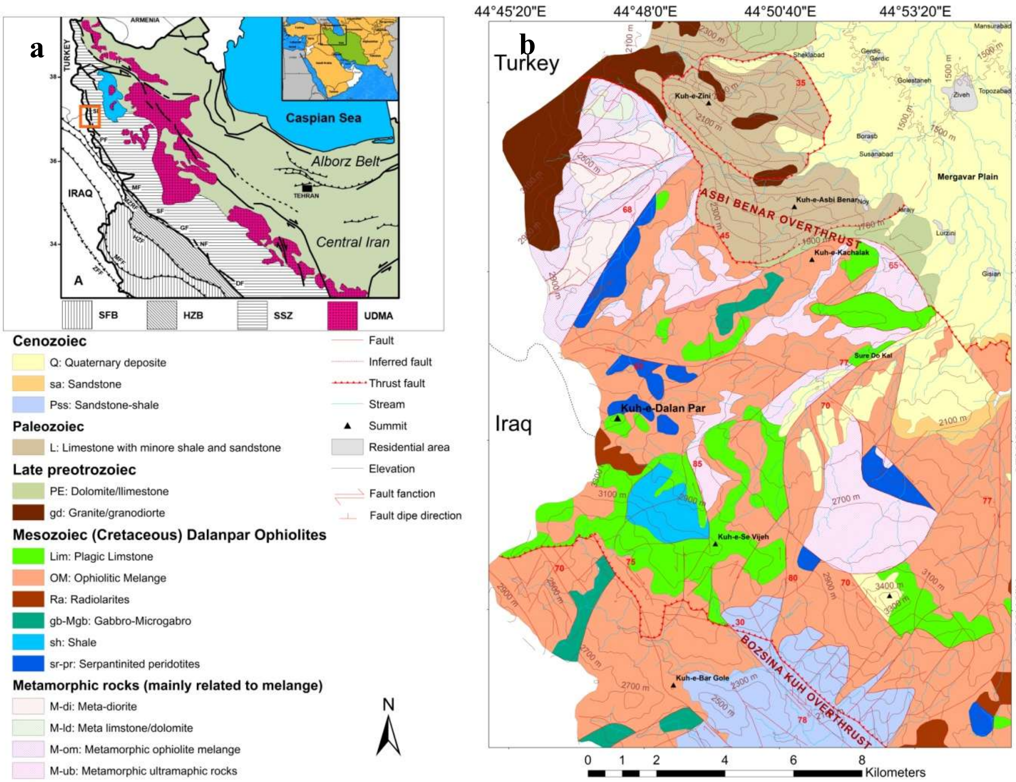

Figure 1. General map of the study area in NW Iran; (a) the Main Recent Fault (MRF) and its segments along the Zagros collision zone (after Mohajjel and Rasouli, 2014). Several segments of the MRF (Tchalenko and Braud, 1974) including Dorud (DF), Nahavand (NF), Garoon (GF), Sahneh (SF), Morvarid (MF) and Piranshahr (PF) faults are shown. The location of the study area is marked in the NW part of the map. The other major faults are Serow Fault (SF), Salmas Fault (S), Tabriz Fault (TF) and the Main Zagros Reverse Fault (MZRF). High Zagros Belt (HZB), Simply Folded Belt (SFB), Sanandaj-Sirjan Zone (SSZ), Urumieh-Dokhtar Magmatic Arc (UDMA) are also shown, and (b) simplified geological map of the Dalanpar Mountains area.

2.2. Methodology

The first step in producing accurate landslide zonation maps involves identifying the factors that influence landslide susceptibility. Considering previous research (e.g., Kamp et al., 2008; Guo et al., 2015; Myronidis et al., 2016; Ghobadi et al., 2017; Eslami et al., 2019; Bahrami et al., 2020) and the landslide characteristics of the study area, seven fundamental conditioning factors that impact landslide susceptibility were identified. These factors include lithology, faults, slope gradient, slope aspect, distance from stream, precipitation, and land use (Fig. S1). To create the slope gradient, aspect, and drainage network layers, a 12.5 m DEM of the study area was employed within ArcGIS software. The lithology and fault data of the study area were obtained from a 1:100,000 geological map of Serrow (Hajolla ali et al., 2005). The precipitation data were obtained from the Iran Meteorological Organization, and the land use map was extracted using satellite images.

Landslide: In this study, a number of multiple or complex landslides were identified, and their locations and boundaries were verified using various sources such as historical records, 1:25,000 topographical maps, Google Earth™ images, 1:100,000 geological maps, and field surveys (Fig.

2). In addition to these sources, the identification and delineation of the study area landslides also relied on geomorphological evidence and drainage features. The geomorphological evidence of the Dalanpar landslides includes irregular, step-like, and hummocky slope morphology, over-steepened crown scarps, bowl-shaped forms of downslope areas, linear ridges that run parallel to contours at the downslope edge of the rotated landslide block, and tension cracks near the head scarp of the landslide (Fig. 3a, b). These cracks are perpendicular to the direction of ground movement, as depicted in Figure 3.

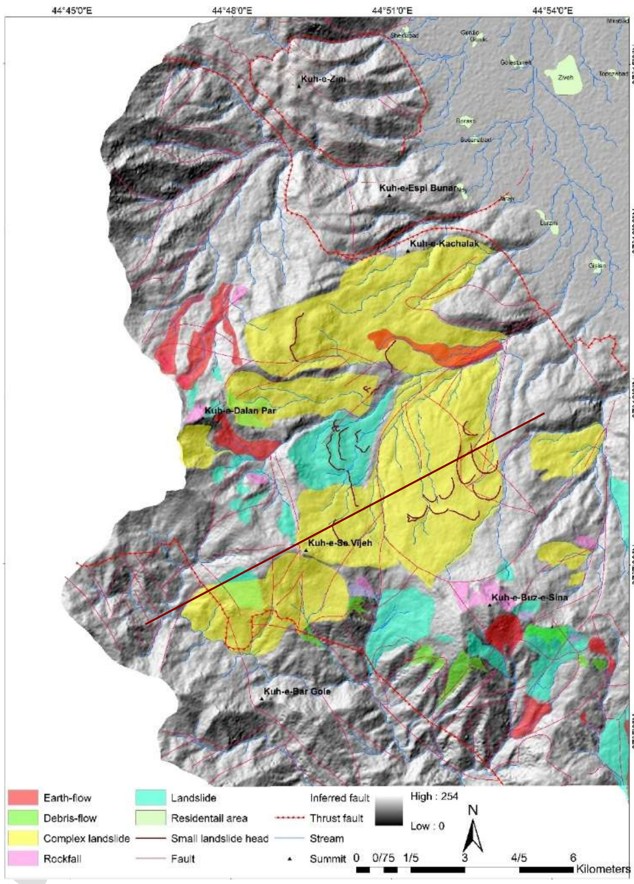

Figure 2. Landslide inventory map of the study area. Landslides are classified according to Varnes (1978) classification.

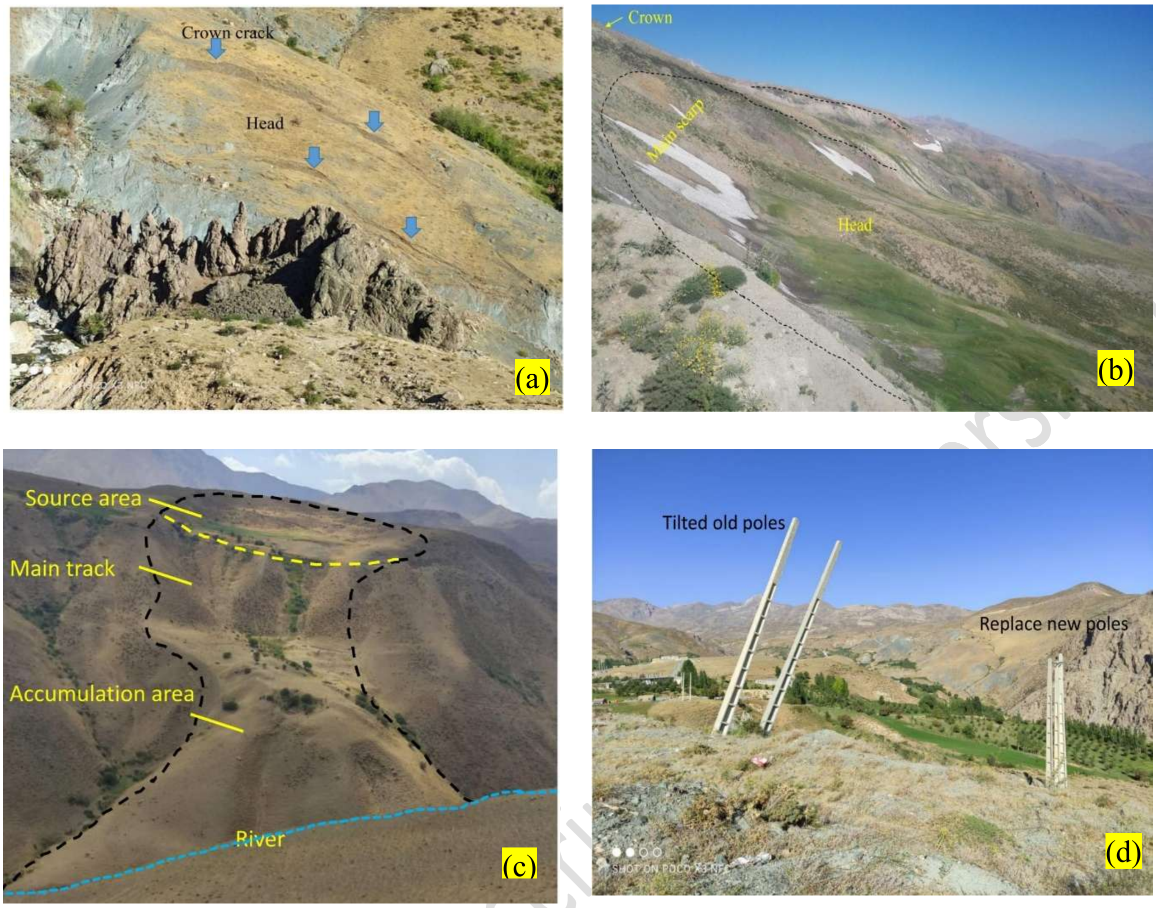

Figure 3. (a) Tension cracks perpendicular to the topographic slope on the apex area south of Sure DoKal young landslide. (b) One of the landslides in the largest complex of Dalanpar Mountains with the over-steepened crown scarps (Note the blue parts, which are often serpentinite). Position of photo: 37° 8'56.36"N and 44°52'55.96"E. (c) A typical intact landslide in the east of the study area with preserved source area, main track and accumulation zone. (d) Bending the newly installed electric poles in the serpentinite unit and replacing them with the right poles.

Lithology and Faults: Lithology and the main effective faults of the Dalanpar region were identified based on geological maps. The existence of these faults was also confirmed during fieldwork. In total, it was found that there are two types of effective faults in the region: thrust faults such as Bozsina and Asepi-Benar overthrusts, and strike-slip faults (MRF), which have had a significant impact on the formation of the regional geomorphology. The role of lithology in landslide occurrence is very clear. The near-fault zone is often characterized by hillslopes with steep slopes and large local relief compared to the surrounding area, creating conducive topographic conditions for the occurrence of landslides. Therefore, in this study, the effect of faults on landslide occurrence was investigated by measuring distance from the faults. The distance from faults map was classified into three buffer zones: 0-500 m, 500-1000 m, and > 1000 m (Fig. S2b).
Slope: Mass movement frequently occurs where the slope is steeper than the natural angle of repose of the substrate, and when there is not enough cohesion to resist slope failure (Kamp et al., 2008). To extract the slope angle in the study area, the ALOS DEM with a 12.5 m resolution was employed. The slope angle map was classified into eight categories: 0-5°, 5-10°, 10-20°, 20-30°, 30-40°, 40-50°, 50-60°, and > 60° (Fig. S2c).

Slope Aspect: Slope aspect plays a crucial role in landslide occurrence since it influences multiple factors such as exposure to sunlight, weathering, precipitation, snow meltwater, land cover, and soil conditions (Bahrami et al., 2020). To extract slope aspects in the study area, a DEM with a 12.5-m spatial resolution was employed, and slope aspects were classified into nine categories: flat (-1°), north (0-22.5°, 337.5-360°), northeast (22.5-67.5°), east (67.5-112.5°), southeast (112.5-157.5°), south (157.5-202.5°), southwest (202.5-247.5°), west (247.5-292.5°), and northwest (292.5-337.5°) (Fig. S2d).

Distance from Stream: Streams play a role in slope stability by causing erosion at the slope toe and saturating the lower part of the slope, resulting in an increase in the water level (Guo et al., 2015; Myronidis et al., 2016). Therefore, to evaluate the impact of streams on landslides, three buffer zones were established with distances of 0-100 m, 100-300 m, and > 300 m from the stream (Fig. S2e).

Precipitation: The role of precipitation in triggering landslides is widely acknowledged, as it can influence soil moisture content, saturation, and pore-water pressure (Wang et al., 2014; Myronidis et al., 2016). To assess its impact on landslides, an average annual precipitation map was generated based on the synoptic stations of West Azarbayjan Province (Iran Meteorological Organization). The average annual precipitation of the study area, spanning from 1986 to 2020, was categorized into three classes: 500-600, 600-700, and 700-810 mm/year (Fig. S2f) (https://www.irimo.ir).

Land Use: Land cover impacts soil moisture and mechanical behavior. Plants can help prevent landslides as their roots act like natural anchors and help manage soil moisture. However, deforestation, road construction, hillside modification, or building construction on slopes can make areas more susceptible to landslides, especially during heavy rainfall (Pacheco Quevedo et al., 2023). The study area's land use maps were obtained using Landsat 8 images from 2020 with a spatial resolution of 30 × 30 m. ENVI 5.3 was used for analysis, employing a supervised classification method with the maximum likelihood algorithm. The land-use classes, including areas, good rangelands, poor rangelands, agricultural lands, and water bodies, were defined (Fig. S2g). Training data were gathered through field surveys, Google Earth images, and previous land-use maps.

Landslide Hazard Zonation: To create a landslide hazard zonation map, a bivariate statistical method was used. This involved comparing the driving factors of landslide hazard with the landslide distribution map as independent (lithology, slope gradient, slope aspect, distance from fault, distance from stream, precipitation, and land use factors) and dependent (landslide distribution map) variables. Two bivariate statistical methods (LNRF and density area) were employed in ArcGIS software for the landslide zonation mapping. The LNRF and Density area methods provide several advantages in landslide hazard assessment. They offer a quantitative measure of landslide hazard, allowing for objective and consistent evaluation across different regions. This helps planners and policymakers prioritize resources and mitigate hazards. Also, these methods use different factors simultaneously, capturing the complex interactions that contribute to landslide occurrence. By incorporating slope characteristics, geological properties, precipitation, land cover, and proximity to rivers, these methods provide a comprehensive understanding of landslide hazard. Additionally, these methods use readily available data, such as digital elevation models, lithology maps, land cover, and rainfall data. This availability makes them suitable for areas with limited data, enabling broad application in diverse geographical contexts. Such methods also allow for the identification of high hazard zones within an area, aiding in the development of hazard maps and land use planning strategies (Bahnassy, 2023).

The approach used in this study involves the calculation of landslide density for each factor map using Equation (1), which is then used to create the landslide hazard zonation map (Lee and Kyungduck, 2001).

$$W = 1000\left[\frac{A}{B}\right] - 1000\left[\frac{C}{D}\right]. \ (1)$$

Where W represents the weight for each class of factors, A is the number of landslides in each class, B is the number of each class, C is the number of landslides in the entire study area, and D is the total number of all classes.

The LNRF (Landslide Numerical Risk Factor) method, which was proposed by Gupta and Joshi (1990), is a bivariate statistical approach. After identifying the influential factors in landslide occurrence, each factor was linked with the landslide distribution maps to quantify the landslide density in each class. The class rate of each factor was determined using Eq. (2) in this method.

$$LNRF = \left[\frac{A}{Average}\right]. \ (2)$$

Following the identification of effective factors in landslide occurrence, each factor was combined with the landslide distribution maps to determine the amount of landslide in each class. The class rate of each factor was determined using Eq. (2), where LNRF represents the Landslide Numerical Risk Factor value, a denotes the landslide area in each class, and Average is the average of landslide area in all classes of each factor. After computing the LNRF of the classes of each factor, the weight of each class was determined according to Table 1.

Table 1. Weight of classes in the LNRF model.

LNRF	Weight
<0.67	0
0.67-1.33	1
>1.33	2

Finally, the landslide hazard zonation map of the study area was generated using density area and LNRF methods and classified into five hazard classes: very high, high, medium, low, and very low. To compare different hazard classes, the density ratio (Dr) was used in each of the hazard classes. To evaluate the models, the quality sum index (Qs), Eq. (3) was used:

$$Qs = \sum_{i=1}^{n}((Dr-1)^2 * S). \ (3)$$

where Qs is quality sum, Dr is density ratio, S is area of hazard class divided by total area, and n is number of hazard classes.

$$Dr = \frac{\frac{S_i}{A_i}}{\frac{\sum_i^n S_i}{\sum_i^n A_i}}. \ (4)$$

According to Eq. (4), Si is the sum of landslide areas of each hazard class, Ai is the area of hazard class number i in a zonation map, and n is the number of hazard classes.

In a zonation method, a hazard class with a density ratio (Dr) of 1, meaning it has a density equal to the average landslide density of the entire region, and a class density ratio of 2, will have a landslide density equal to two times the density of the region. Simply put, the higher the Qs of a landslide hazard zonation map, the greater its accuracy (Gee, 1991).

For further validation and based on the results and observations, a receiver operating characteristic curve (ROC) was prepared for a quantitative accuracy assessment. ROC is a standard technique to validate the accuracy of a classifier that can be used for validation of landslide susceptibility models. ROC is a graphical plot that explains the performance of a binary classifier model at varying threshold values.

3. Result

3.1. Lithology

The mass movement distribution map of the study area portrays various types of slips, such as earth flow, debris flow, landslide, rock fall, and complex landslides that have been continuously active from the past to the present (Fig. 2). The Dalanpar landslides cover an area of approximately 280 km². Within the Dalanpar Mountains, seven sub-zones with multiple landslides were identified and classified into seven complex landslides (Fig. 2). These complexes include many landslides, earth flows, debris flows, and rockfalls, some of which occurred in several stages. Additionally, numerous separate landslides of various sizes are also observed in the study area. Most of the large and multiple landslides are situated on the eastern side of the Dalanpar Mountains, while the landslides on the western side are typically smaller, younger, and more intense events. The lithological units in the study area include L, Lim, M-di, M-om, M-ub, OM, PE, Pss, Q, Ra, gd, sa, sh, and sr-pr (Fig. 1b). The ophiolite complex dominates most of the study area (Fig. 1) and comprises various units ranging from ultramafic to intrusive and extrusive basic rocks. The primary mineral in the ophiolite complex, particularly in ultramafic units, is olivine. However, olivine is unstable on the earth's surface due to the significant difference between the location of its formation and the earth's surface conditions. When olivine minerals and pyroxenes absorb water on the ground surface, they transform into serpentine minerals, which have a slippery nature and a soapy luster despite the absorbed water (Morgan and Ranero, 2023). Serpentinization is highly prevalent in the Dalanpar ophiolites. In the ophiolite sequence, peridotites are typically located at the lower level. Hence, instability at the bottom of a structure can lead to instability in the upper parts. Serpentinization is a trigger factor for landslide occurrence in the ophiolitic complex, although the slope gradient of the ophiolitic complex also has a significant impact on the occurrence of landslides (Bahrami et al., 2020; Morgan and Ranero, 2023). For instance, no landslide has been observed in the ophiolites of Kermanshah (Saccani et al., 2013) and Neyriz, where their slopes are less than 20° (Monsef et al., 2018).

3.2. Tectonics

Orogenic regions are characterized by the presence of thrust faults, strike-slip faults, and normal faults, which are clearly visible in the Dalanpar area (Fig. 1). The Bozsina thrusts with dips of about 35° to 40° to the NE in the north and Espībenār thrusts with dips of 30-40° to the NE in the southern part of the study area are the most prominent faults (Fig. 1). These thrusts run parallel to the main Zagros fault, which is observed in the western region of the studied area (Fig. 1a). These thrusts have had a significant impact on the disruption of ophiolite units, resulting in their obduction to an altitude of 3500 m a.s.l. Numerous reverse faults have formed in parallel with these thrusts, causing the units' boundaries to be predominantly fault-controlled. This has led to severe fragmentation of the units and made the peridotites highly reactive to serpentinization. It is noteworthy that the slope gradient is the result of the compression caused by these thrust faults, which has led to a significant slope inclination in the mountainside and the formation of these mountains.

One of the major types of faults in the region are dextral strike-slip faults, which have emerged over the last ten million years as a result of the dextral slip component of the Zagros Main Fault (Tchalenko and Braud, 1974; Talebian and Jackson, 2002; Mohajjel and Rasouli, 2014; Rahimzadeh et al., 2019). This fault is oriented at an angle of around 30 degrees along the Zagros thrust and has an extension of approximately 330 degrees, intercepting most of the regional thrust structures because of its relative youth. The dip of the faults in the study area varies from 60° to 90° towards the northeast, which increases the potential for landsliding in the eastern front of the mountains. The activity of dextral strike-slip faults, mostly with N to NW trend, cuts the lithological units and has further increased the instability and susceptibility to landslides with E-W trend. On the other hand, perpendicular seams, cracks, and fractures caused by strike-slip faults have led to increased permeability and serpentinization in the Dalanpar peridotites, owing to the increased drainage resulting from the fact that the trend of most faults is perpendicular to the general slope gradient of the area. Additionally, these faults sometimes have local extension components like other segments of MRF (Rahimzadeh et al., 2019; Bahrami et al., 2020). Faults also augment the susceptibility to landslides because rocks adjacent to faults are weaker, owing to intense shearing (Leir et al., 2004). Given the significant influence of faults on slope instability, three buffer zones were generated with 500-m intervals to account for the effect of distance from faults on landslide susceptibility (Fig. S2b). Results show that 72.46% of landslide area has occurred within 0-500 m distance from the faults (Table S1).

3. 3. Dalanpar Lakes

A total of 27 lakes were identified in the study area, which were formed as a result of either landslide occurrence, sag ponds, or glacial processes (Table S2). The lakes' sizes varied greatly, with the smallest lake (La14) having an area of 50 m² and the largest lake (La6), known as "Mama Shaikh lake," having an area of 149,778 m². The altitude of these lakes ranged from 1923 to 3183 m a.s.l. While some of these lakes are seasonal, others are permanent (Table S2). Most of the lakes were formed on the upslope of the hummocks in the accumulation zone of landslides (Fig. S3a, b). However, some lakes were located near the young faults and adjacent to the snow ridges that were fed by seasonal snow meltwater (Table S2).

3.4. Landslide Hazard Zonation

Table S1 provides a comprehensive list of the influential factors contributing to landslide occurrences in the study area. Despite the occurrence of various lithological units in the study area, the OM (Ophiolitic Mélange) unit covers a significant portion of the study area (33.37%). The findings reveal that the majority of landslides (70%) took place in the serpentinized ultramafic complexes (Fig. S2a and Table S1) that likely appear prone to sliding due to their high water absorption and soapy polish. The study area is primarily characterized by slope gradients ranging from 10-30 degrees, which account for more than half of the total area, and about 90% of landslides are located on slopes with gradients of 5-30 degrees (Fig. S2c and Table S1). Furthermore, the study area comprises mainly NE (18.57%), N (15.66%), and E (15.33%) slope aspects, with most landslides associated with the northeast, east, and southeast aspects (Fig. S2d and Table S1). Data reveals that a significant proportion of landslides occurred close to fault traces, with 72.46% of the landslide area taking place within a distance of 0-500 meters from the faults (Fig. S2b and Table S1). However, there was no clear correlation between the distance from streams and landslide occurrence (Fig. S2e and Table S1). The evaluation of landslides in the precipitation and land-use classes shows that most landslides occurred in the 600-800 mm precipitation class (Fig. S2f and Table S1) and good rangeland class (Fig. S2g and Table S1). Almost 80% of the study area is covered by rangeland, where most of the landslides have occurred.

The landslide hazard zonation map was generated using the LNRF (Fig. 4a) and density area (Fig. 4b) methods, which were divided into five hazard classes ranging from very low to very high. The results of the LNRF model demonstrate that high and very high hazard zones occupy approximately 36% of the study area, while the density area model shows that high and very high hazard zones cover about 47% of the study area. Moreover, the validation process using the Quality Sum (Qs) index reveals that the density area model with Qs = 0.57 was more precise than the LNRF model with Qs = 0.35 (Table 2). In other words, the density area method outperforms the LNRF method in terms of quality sum.

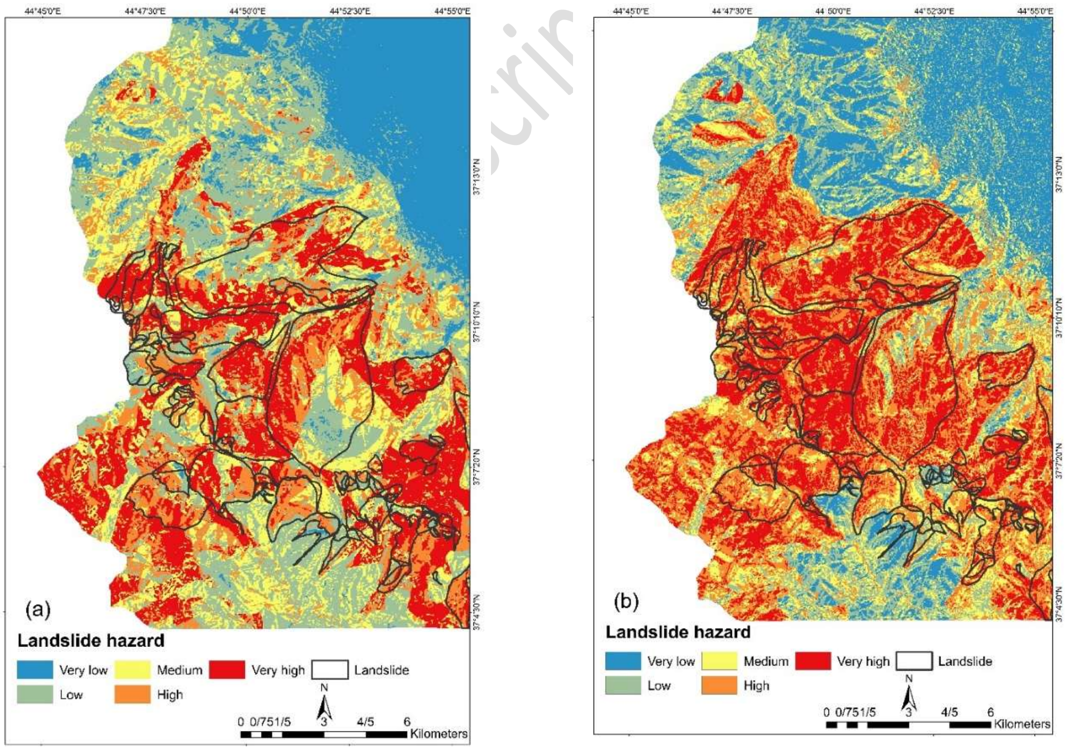

Figure 4. Landslide hazard zonation map by (a) the LNRF method; (b) the density area method.

Table 2. Assessment of LNRF and density area methods.

Models	Hazard zones	(Ai)	(Si)	Si/Ai	Dr	S	Qs = (Dr-1)2*S
LNRF	Very low	50.37	0.76	0.01	0.06	0.17	0.15
	Low	84.12	15.80	0.19	0.70	0.28	0.02
	Medium	60.01	15.44	0.26	0.96	0.20	0.00
	High	43.68	19.16	0.44	1.64	0.15	0.06
	Very High	63.07	29.32	0.46	1.74	0.21	0.11
	Total	301.25	80.46	0.27	1.00	1.00	Qs=0.35
Density area	Very low	59.87	0.58	0.01	0.04	0.20	0.18
	Low	51.11	3.75	0.07	0.27	0.17	0.09
	Medium	48.50	10.32	0.21	0.80	0.16	0.01
	High	73.21	29.17	0.40	1.49	0.24	0.06
	Very High	68.55	36.64	0.53	2.00	0.23	0.23
	Total	301.23	80.47	0.27	1.00	1.00	Qs=0.57

Ai: area of hazard class number i in a zonation map, Si: sum of landslide areas of each hazard class, S: area of hazard class divided by total area, Dr: density ratio, Qs: quality sum.

Based on a combination of field studies and geological maps, the results show that approximately half of the Dalanpar Mountains have been affected by landslides, occurring from the plain bottom to the mountain peaks (Fig. 2). The density area method (Table S1) indicates that the most significant factors contributing to landslide occurrence are the serpentinite unit of the ophiolite (OM, M-ub, sr-pr) and Lim, slope gradients of 60-77° and 5-20°, northeast aspect, 0-1000-meter distance from fault, 0-300-meter distance from stream, 600-810 mm precipitation, and good rangeland use. The LNRF method indicates that the serpentinite unit of the ophiolite (OM, M-ub, sr-pr) and Lim, 0-30° slope gradients, northeast and east aspects, 0-500-meter distance from fault, 600-810 mm precipitation, and good rangeland use are the main factors affecting the landslide occurrence.

4. Discussion

4.1. Hazard Zonation

Field observations suggest that landslides have occurred in various stages, with complex movements that are sometimes difficult to differentiate. However, in some complexes, events can be reconstructed with considerable precision. Landslides in the western part of the mountains are younger and more active than those in the eastern part, with landslides in the complexes of the western part being more dynamic and obvious. Figure 5a illustrates a landslide complex in the western part of the study area, showing three generations of landslides. The first and second generations were composed of considerable movements of materials, creating large steps that formed lakes upslope of the accumulated materials. The volume of transported mass in the first stage was so large that it caused instability and repeated landsliding, which created the second lake at lower altitudes. Following these landslides, earth-flow and rockfall phenomena were created, causing the edge of the second lake to break and flow downstream. A topographic profile of the events (Fig. 5b) demonstrates the slope morphology and a lake developed upslope of a hummock. Lakes are important features of unstable slopes, often suggestive of landslides. Landslides are considered one of the most important factors in the formation of lakes, as driven wedges and stairs created by landslides in steep mountains create bowl-like areas where water can easily collect. Since the annual rainfall of the Dalanpar Mountains is >800 mm and mostly in the form of snow, most lakes have a significant water supply throughout the year.

Fig. 5b

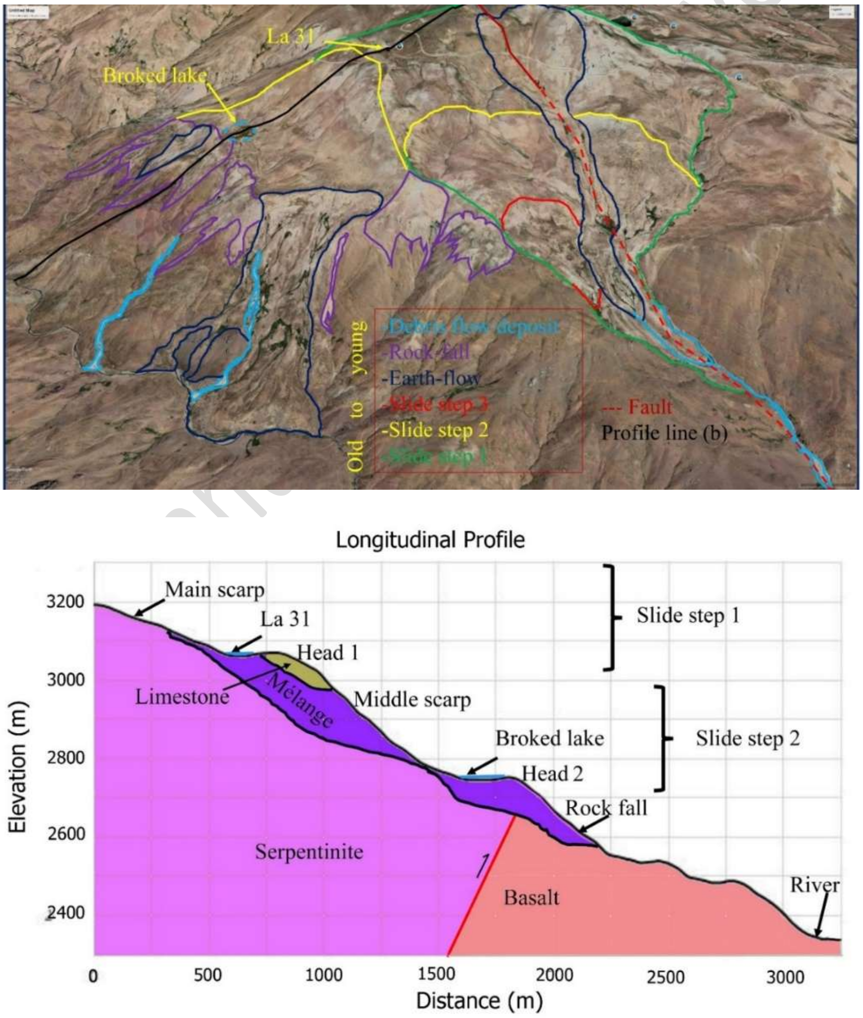

Figure 5. (a) Google Earth image showing one of the west Dalanpar complexes and their occurrence caused by landslides, (b) a topographic cross-section of western part of Dalanpar slope showing the morphology of slope and a lake developed upslope of a hummock.

Over 70% of the landslides in the study area occurred in mélange areas with an ophiolite mélange and the serpentinite matrix (Fig. 1, 4b and Table S1). Most of the landslides in the Dalanpar Mountains happened in the serpentinite units or in the units overlying serpentinite. However, in the south of the village of Surah Dukal (Fig. 6), three generations of landslides have been observed in the serpentinites. The first two generations have been cut off by debris flows, but the third generation of landslides is currently active. This location is a prime example of landslide movements in the Dalanpar Mountains.

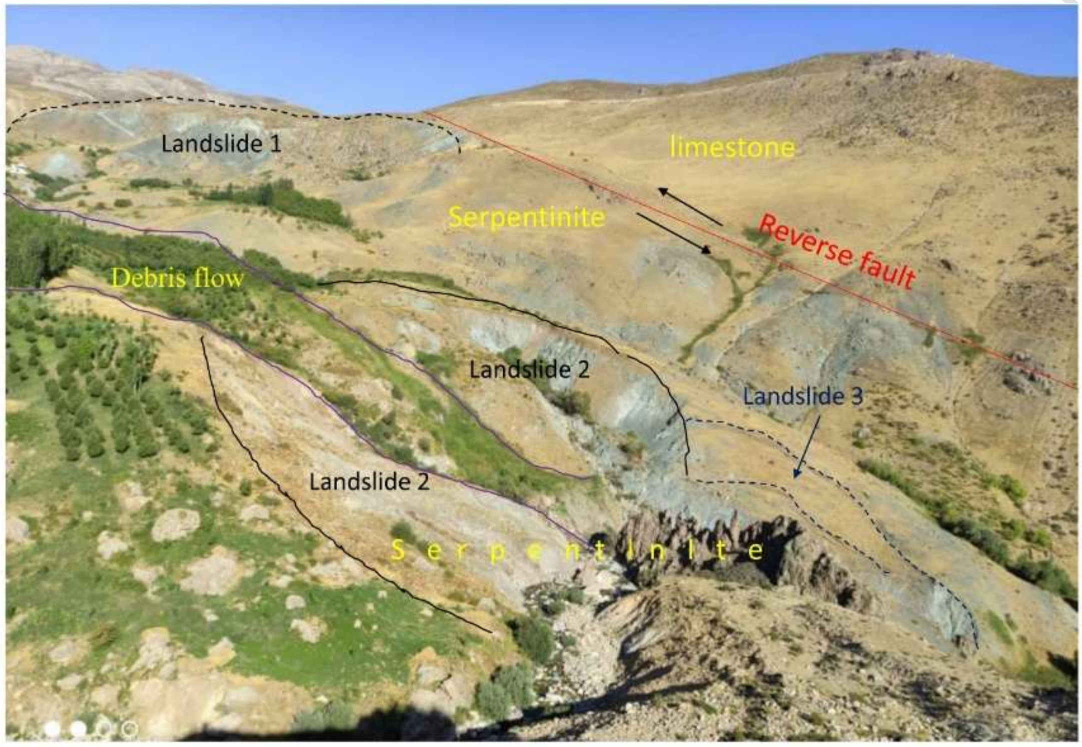

Figure 6. The three generation landslides occurred in the eastern part of the Dalanpar Mountains with thrust fault (Aspi Benar overthrust).

The results indicate that both methods used for landslide hazard zonation have identified similar factors affecting slope instability. The density area method has a higher accuracy and applicability than the LNRF method in predicting landslide hazard, which is consistent with previous studies by Ghobadi et al. (2017) and Eslami et al. (2019). Additionally, the results of both methods suggest that the combination of all factors has contributed to landslide occurrence in the Dalanpar Mountains. Furthermore, the success rate curves (Fig. 7) show cumulative percentage of observed landslide occurrences versus cumulative areal percentage of decreasing landslide susceptibility index value for the density area method (a) and LNRF method (b). The area under the curve (AUC) is 72% for the density area method and 68% for the LNRF method, implying overall success rates of the landslide susceptibility zonation maps for the mentioned methods.

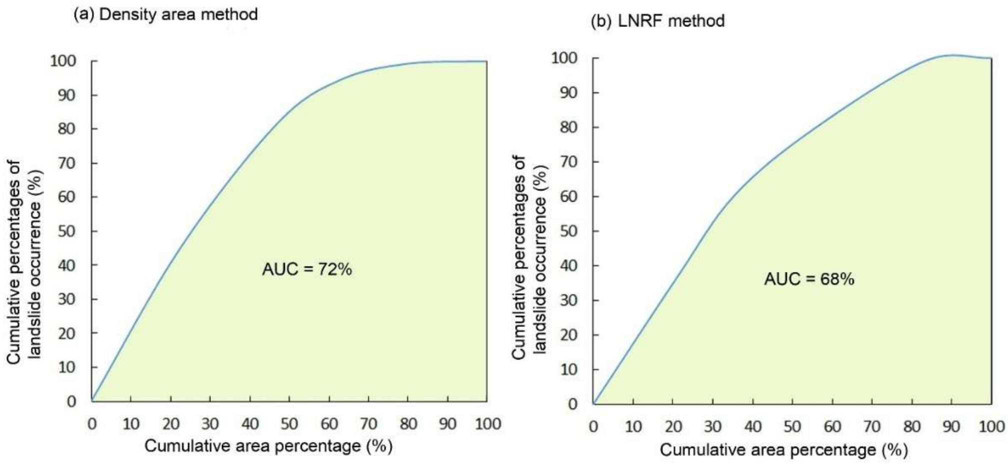

Figure 7. The success rate curve showing cumulative percentage of observed landslide occurrences versus cumulative areal percentage of decreasing landslide susceptibility index value for density area method (a), and LNRF method (b). The area under curve (AUC) is 72% for density area method and 68% for LNRF method, implying overall success rate of the landslide susceptibility zonation map for mentioned methods.

In the Dalanpar Mountains, high slope gradients and precipitation can be considered as hazardous elements that contribute to landslides. Precipitation is an external factor that triggers landslides (Hamza and Raghuvanshi, 2017), as it affects the water content of the soil, soil saturation, and pore-water pressure (Guzzetti et al., 2008a, b; Bahrami et al., 2020). The study area receives a substantial amount of annual precipitation (about 800 mm/year) compared to the mean annual rainfall of Iran (240 mm) (Soltani et al., 2012), which is an important factor that facilitates landslide occurrence in the Dalanpar Mountains. Additionally, results show that most landslides have occurred on the northeast slope aspect, which is in line with the findings of Ghobadi et al. (2017) and Kahal et al. (2021), suggesting that most landslides have occurred on the north (N), northwest (NW), and northeast (NE) aspects.

4.2. Serpentinization Effect

Results show that the occurrence of landslides is strongly associated with the exposure of serpentinites that are cut by faults (Fig. S2a), as indicated by the majority of landslides in the region. Serpentinite units are widely distributed throughout the different geological formations, although they are mostly covered by variable units and soil. This highlights the significant influence of serpentinite units in the formation of major landslides, particularly in landslide complexes (Fig. 2, 5a). The overlying units of the serpentinites consist mainly of basalt, limestone, shale, and radiolarite. As the serpentinites are located beneath these rock units, they act as heavy objects on a slippery and loose matrix, thus facilitating more landslides due to their weight.

The alteration process of peridotites occurs rapidly and easily under surface conditions through the hydration of silicate minerals such as olivine and pyroxene, which are major components of ultramafic units like peridotites (Neumann et al., 2015). The instability of these minerals at the surface is due to differences in temperature and pressure compared to their conditions during formation. Serpentinites, which are produced from the peridotites, are primarily composed of three minerals: lizardite, chrysotile, and antigorite (Fig. 8). The serpentinization process involves OH in all of these minerals and releases iron, calcium, and silica as secondary minerals in veins and fractures. The process of serpentinization occurs when ultramafic rocks enriched with olivine and orthopyroxene minerals react with water and are converted into rocks containing a set of minerals dominated by serpentine. H_2 is an important by-product of this reaction. The alteration process in peridotites can occur easily and quickly under surface conditions through the hydration of silicate minerals such as olivine and pyroxene, which are the main minerals of ultramafic units like peridotites (Neumann et al., 2015). These minerals are unstable at the surface due to the difference in their formation conditions, particularly in terms of temperature and pressure. During the process of serpentinization, ultramafic rocks react with water and a set of serpentine minerals is formed, and H_2 is produced as a by-product (Preiner et al., 2018). Serpentine minerals have a soapy polish and are also known as soapstone, as they are very slippery due to their fibrous and filamentous growth. Additionally, the absorption of water in the structural formula and mineral layer of serpentinites can make them twice as slippery.

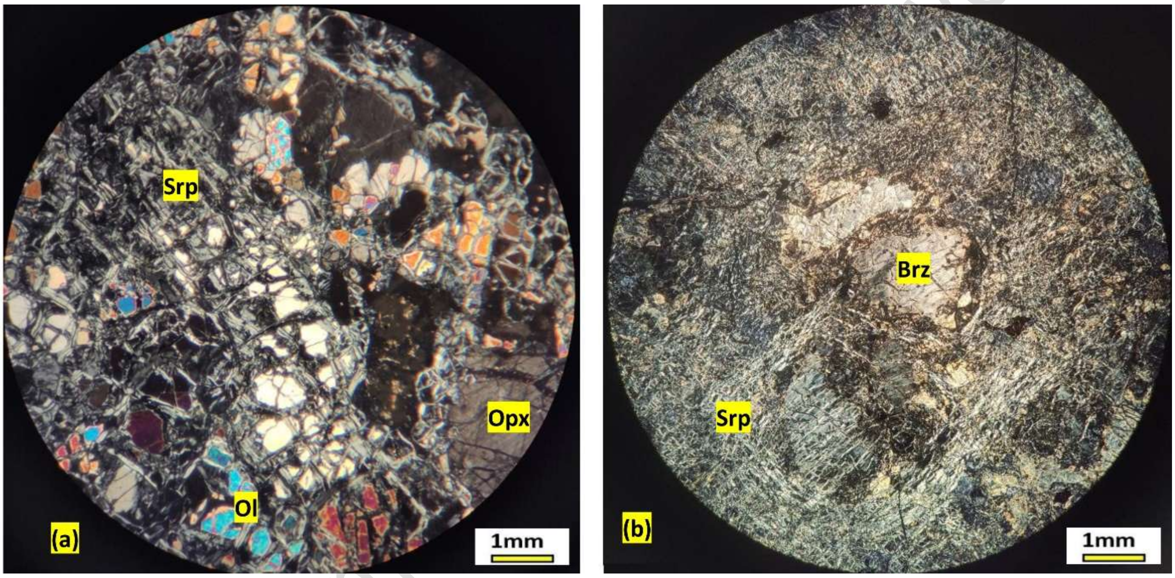

Figure 8. The microscopic photos from serpentinization process in Dalanpar peridotite rocks where the olivine changed to serpentine minerals and orthopyroxene to bronzite. (a) serpentinized dunite (reaction is ongoing) and (b) serpentinite (reaction is complete). (Ol: olivine; Opx: orthopyroxene; Srp: serpentine; Brz: bronzite).

4.3. Tectonic Effect

Tectonically active orogenic belts, such as the Zagros region, frequently exhibit active faults with diverse mechanisms (Tchalenko and Braud, 1974; Alavi, 1994; Mohajjel and Rasouli, 2014). Among the most significant faults in the Zagros are the main Zagros fault, characterized by thrust structures and a northeast slope, northeast-southwest-trending normal faults, and the strike-slip Main Recent Fault of Zagros, which has a relatively high slope (Rahimzadeh et al., 2019). These faults can facilitate landslides in ophiolite complexes in several ways.

Firstly, they cause the slicing and crushing of rock units, especially peridotites, creating an effective contact surface for alteration and serpentine reactions (Melosh, 2019; Aupart et al., 2021). Secondly, they enhance the movement of water throughout the unit, which promotes the serpentinization process and causes water to penetrate the lower sections, facilitating the movement of rock masses. Thirdly, on steep slope surfaces, fault sections, especially where fault directions are almost coincident with the topographic slopes, can facilitate downstream movement of rock masses, such as in the case of landslides in the Sarvabad region (Bahrami et al., 2020). Finally, earthquakes induced by faults result in sudden and powerful movements, and most large landslides are caused by such a driving force (Harrison and Falcon, 1937; Tibaldi et al., 1995; Shoaei and Ghayoumian, 1998; Parker et al., 2015; Liu et al., 2021).

Earthquakes are secondary effects of faults affecting the occurrence of Dalanpar landslides. The distribution of historical earthquake data in Dalanpar and the surrounding area (Fig. 9) indicates that this region is highly seismic, and these earthquakes have had an impact on the triggering and occurrence of landslides (Fig. 9).

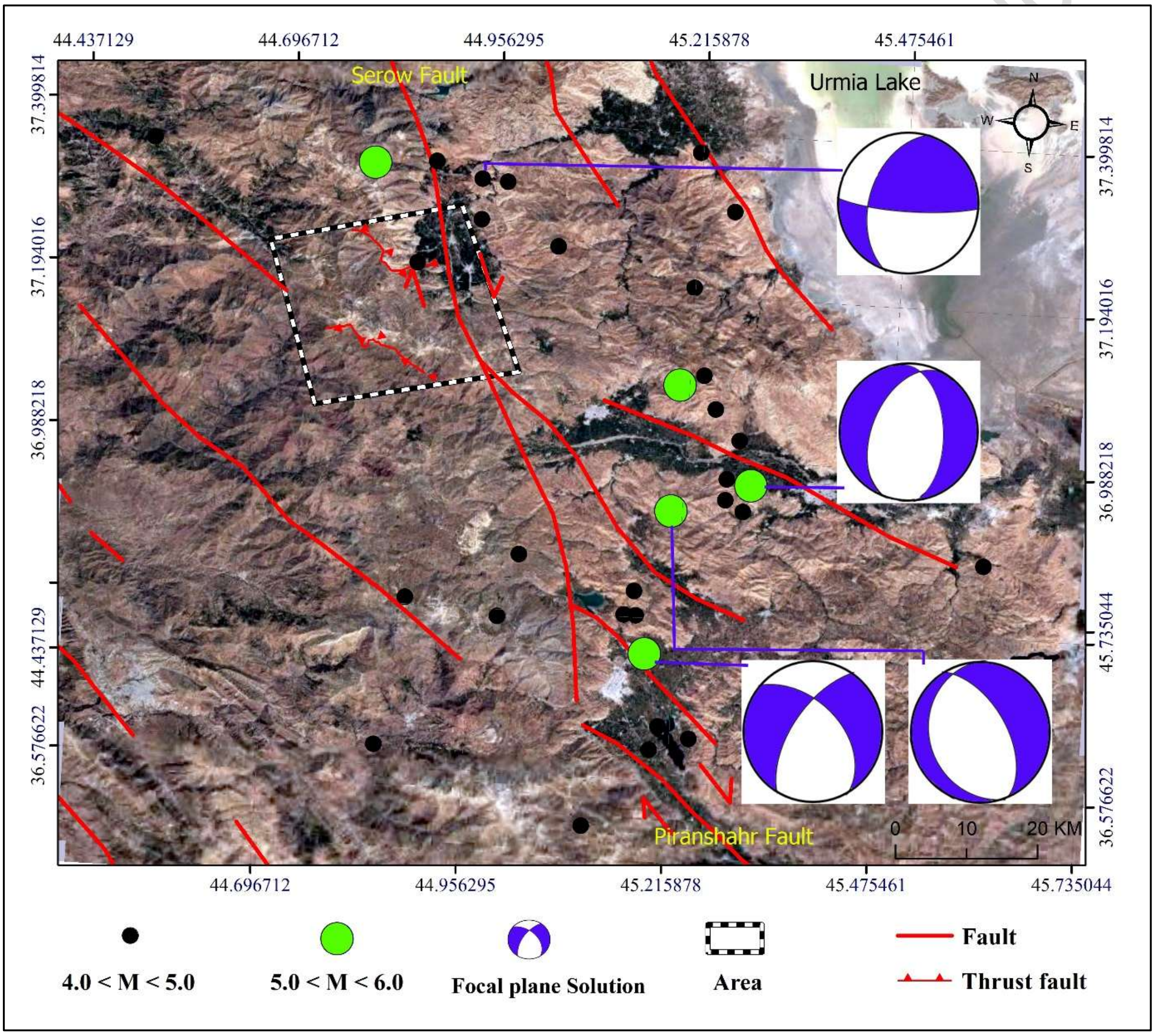

Figure 9. The focal plan solution of the Dalanpar area and surrounding.

4.4. Evolution of lakes

Lakes are known as one of the phenomena that can form after the occurrence of landslides and can be divided into two types in terms of their formation mechanism: first, by damming the channels of rivers, and second, by accumulation of water behind the pushed mass of the slides. Dalanpar lakes fall into the second group. Evaluation of the morphology of the Dalanpar Mountains shows that landslide-induced lakes are the most important geomorphological evidence of landslide activity (Fig. 10). However, the effect of dextral strike-slip faults cannot be ignored, and seasonal glaciers have also played a role in their evolution (Fig. 10). Lakes formed by landslides are more likely to be dammed by rivers (Nicoletti and Parise, 2002; Zhou et al., 2019). However, the lakes of Dalanpar have developed upslope of landslides, and some of them may be thousands of years old. Compared to other landslide sites (e.g., Bahrami et al., 2020), the number and size of the lakes in Dalanpar are much larger and more extensive.

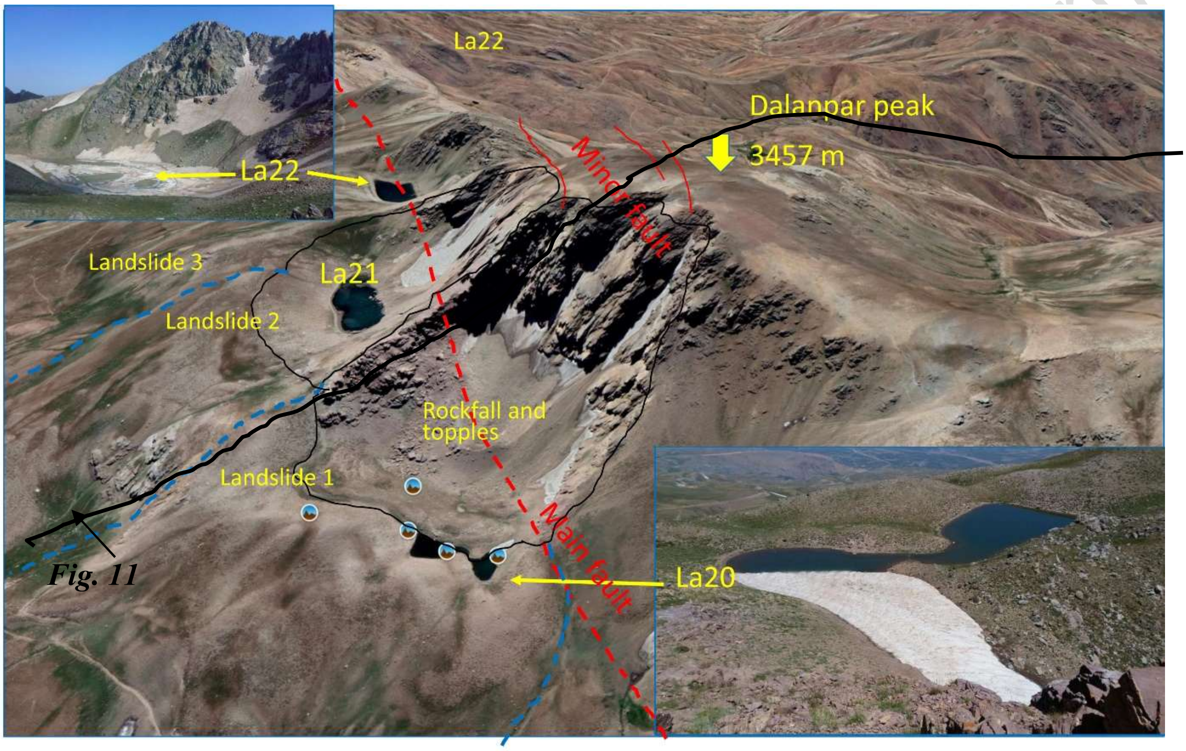

Figure 10. Relationship of linear lakes formation with landslides and also Normal fault effect.

4.5. Geodynamic Model

During the peridotite to serpentinite reaction, the volume of the resulting product increases, causing a decrease in density and driving the serpentinite towards the surface. This movement leads to the penetration of the overlying units, carrying fragments of these units in an exotic form and floating, similar to the process of diapirism observed in salt domes (Talbot and Jackson, 1987; Koyi, 1998). The serpentine acts as a mesostasis and causes disintegration and disruption in the ophiolitic sequence while moving towards higher levels (Stocklin, 1990). The process can take a long time depending on the rate of the reaction and the original volume of the peridotite. The reaction is exothermic and results in an increase in temperature, which helps in the formation of diapirs and metamorphism of rock units at the green schist facies level.

In the Dalanpar Mountains, as a result of orogeny after the collision, the compression system cannot accommodate a large volume of serpentine, but the young dextral fault of Zagros, formed during the last ten million years, and the local extensional basins of the MRF fault in Zagros can provide suitable locations for serpentine diapirs to rise to the surface (Tchalenko and Braud, 1974; Rahimzadeh et al., 2021). The upward and bilateral exit can lead to the formation of a positive flower system, which best explains the uplift and continuous movements of Dalanpar Serpentinites in the mountain. The outcrop of serpentinite is not completely symmetrical in Dalanpar Mountain and tends towards the east, consistent with the direction of the orogenic force of Zagros from southeast to northeast. This asymmetry can explain the frequency and development of landslides in the eastern slope of Dalanpar (Fig. 11).

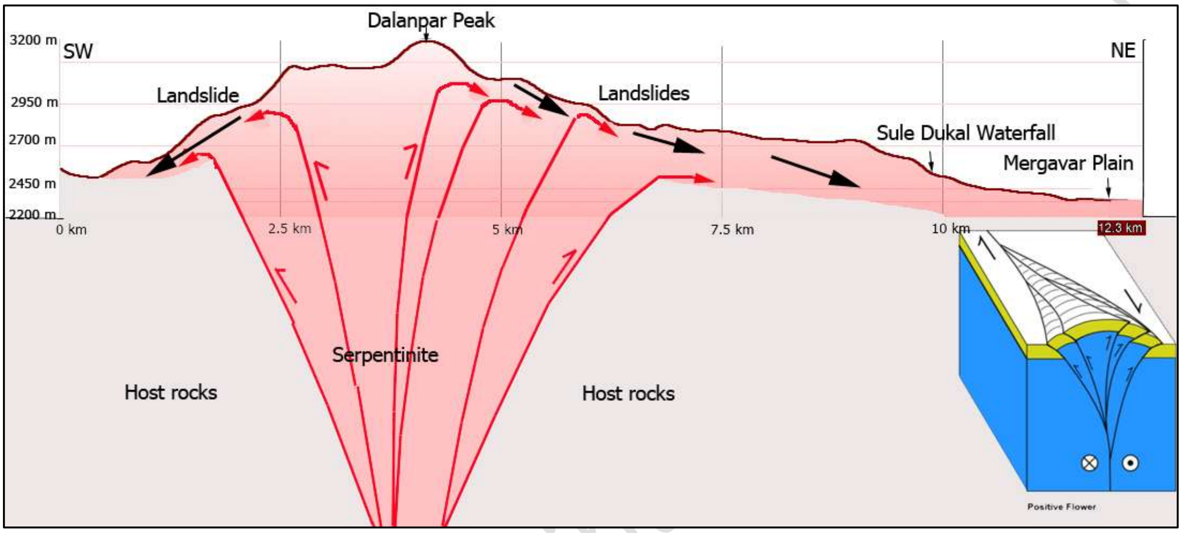

Figure 11. A schematic model depicts the formation of Delanper Mountain and the subsequent development of its landslides in a diapiric system, influenced by dextral strike-slip faults and the creation of the positive flower structure.

The continuous driving force of diapirism has increased the height of Dalanpar Mountain, but the slippery features of serpentinites at high altitude have also caused instability, resulting in domain movements with different dimensions, particularly landslides. With the young Zagros fault's activity and the significant volume of Dalanpar serpentines on the Iran-Iraq-Turkey border, the process of diapirism is ongoing, and its progress to higher levels causes continuous surface movements and deformations. As a result, it is predicted that the landslides of Dalanpar Mountain will continue for thousands and even millions of years to come.

The ascent of serpentinites by the mechanism of diapirism, from the lower layers to the surface of the earth and its elevation, has been studied (Stocklin, 1990). On the other hand, the existence of landslides in areas with widespread serpentinites is well known (Gibson et al., 1996; Fioraso et al., 2019). However, the missing link is how the triangle of serpentinization-diapirism-landslides is connected.

For the first time in this research, we propose an explanation for the high elevation of the Dalanpar Mountains, despite the very strong erosion of serpentinite lands. We also explain why successive generations of landslides have occurred, which is the result of continuous elevation due to the uplift of the low-density and hot mass of serpentinites. The continuous activity of the diapirism system causes a continuous increase in height and slope, resulting in the frequent occurrence of landslides (Fig. 11).

5. Conclusion

- Dalanpar Mountain has a serpentinite matrix (with exotic limestone, basalt, and gabbroic fragments) in which many mass movements have occurred in successive generations and are still highly active.
- Factors of geology (lithology, fault), slope, slope aspect, precipitation, and land use are the triggering parameters in the occurrence of landslides. Most of the landslides have occurred in serpentinized ultramafic complexes and Ophiolitic Mélange, on slope gradients of 5-30 degrees, with northeast, east, and southeast slope aspects, and close to fault traces. However, there was no clear correlation between the distance from streams and landslide occurrence. The evaluation of landslides in the precipitation and land-use classes shows that most landslides occurred in high precipitation and good rangeland classes. The landslide hazard zonation maps and their validation reveal that the density area model was more precise than the LNRF model.
- Although general factors such as slope, precipitation, etc. have effects on the occurrence of landslides in Dalanpar Mountain, the most important factor in the occurrence of landslides is serpentinization. The active tectonics of right-lateral strike-slip faults are the second most important cause of landslides. Neighboring mountains with similar slope, topography, and precipitation are devoid of any landslides.
- The activity of the active tectonic system (branches of the young Zagros fault such as Piranshahr and Servo) has caused many earthquakes in the region. Therefore, earthquakes are another important factor in the occurrence of landslides. Although we would expect the occurrence of landslides to reduce the height of the Dalanpar Mountains, they are equal in height to the neighboring granites and limestones without landslides, which is due to the ascent of serpentinites in a plume-like system.
- The continuous activity of landslides over long periods is due to the continuous feeding of the diapiric system, which continuously pushes the serpentinite upwards like a paste. A total of 27 seasonal and permanent lakes have formed in Dalanpar, all of which are located upslope of the landslides and on the mountain slopes at an altitude of 2000 to 3100 meters. Seasonal glaciers have further developed these lakes and supply them with water during the warm season.

Acknowledgements
The authors would like to express their warmest thanks to Professor John Clague, Editor-in-Chief of Natural Hazard Journal, for his effective comments in structuring and improving the manuscript. The authors also express their sincere gratitude to Rezgar Mollazadeh and his family for their invaluable assistance during two stages of field observations conducted in 2018 and 2021.

Disclosure statement

No potential conflict of interest was reported by the authors.

Data availability
The data that support the findings of this study are available from the corresponding author, upon reasonable request.

References

Agard P., Jolivet L., Goffe B. (2001) Tectonometamorphic evolution of the Schistes Lustres Complex; implications for the exhumation of HP and UHP rocks in the Western Alps. *Bulletin de la Société géologique de France* 172(5): 617-636. DOI: https://doi.org/10.2113/172.5.617

Alavi M. (1994) Tectonics of the Zagros orogenic belt of Iran: new data and interpretations. *Tectonophysics* 229: 211–238. DOI: https://doi.org/10.1016/0040-1951(94)90030-2

Aupart C., Morales L., Godard M., Jamtveit B., the Oman D. P. Science Team (2021) Seismic faults triggered early stage serpentinization of peridotites from the Samail Ophiolite, Oman. *Earth and Planetary Science Letters* 574, 15: 117–137. DOI: https://doi.org/10.1016/j.epsl.2021.117137

Bahrami S., Rahimzadeh B., Khaleghi S. (2020) Analyzing the effects of tectonic and lithology on the occurrence of landslide along Zagros ophiolitic suture: a case study of Sarv-Abad, Kurdistan, Iran. *Bulletin of Engineering Geology and the Environment* 79: 1619–1637. DOI: https://doi.org/10.1007/s10064-019-01639-3

Bahnassy M. H. (2023) Evaluation of Landslide Risk with the Landslide Numerical Risk Factor (LNRF) Method. *Journal of Geology & Geophysics* 12:1114. DOI: https://doi.org/10.35248/2381-8719.23.12.1114

Carlini M., Chelli A., Vescovi P., Artoni A., Clemenzi L., Tellini C., Torelli L. (2016) Tectonic control on the development and distribution of large landslides in the Northern Apennines (Italy). *Geomorphology* 253: 425–437. DOI: https://doi.org/10.1016/j.geomorph.2015.10.028

Christaras, B. (1997) Landslides in iliolitic and marly formations. Examples from north-western Greece. *Engineering Geology* 47: 57–69. DOI: https://doi.org/10.1016/S0013-7952(96)00123-8

Conforti M., Ietto F. (2020). Influence of tectonics and morphometric features on the landslide distribution: a case study from the Mesima basin (Calabria, south Italy*). Journal of Earth Sciences* 31: 393-409. DOI: https://doi.org/10.1007/s12583-019-1231-z

Cirillo D., Zappa M., Tangari A. C., Brozzetti F., IETTO F. (2024) Rockfall Analysis from UAV-Based photogrammetry and 3D Models of a Cliff Area. *Drones* 8, 31. DOI: https://doi.org/10.3390/drones8010031

Cui S., Pei X., Huang R. (2018) Effects of geological and tectonic characteristics on the earthquake-triggered Daguangbao landslide. China. *Landslides* 15: 649–667. DOI: https://doi.org/10.1007/s10346-017-0899-3

Delgado F., Zerathe S., Schwartz S., Mathieux B., Benavente C. (2022) Inventory of large landslides along the Central Western Andes (ca. 15°–20° S): Landslide distribution patterns and insights on controlling factors. *Journal of South American Earth Sciences* 116: 103824. DOI: https://doi.org/10.1016/j.jsames.2022.103824

Dilek Y., Furnes H. (2014) Ophiolites and Their Origins. *Elements* 10 (2): 93–100. DOI: http://dx.doi.org/10.2113/GSELEMENTS.10.2.93

Eslami M., Shadfar S., Mohammadi-Torkashvand A., Pazira E. (2019) Assessment of density area and LNRF models in landslide hazard zonation (Case study: Alamout watershed, Qazvin Province, Iran). *Acta Ecologica Sinica* 39: 173-180. DOI: https://doi.org/10.1016/j.chnaes.2018.08.001

Fioraso G., Balestro G., Festa A., Lanteri L. (2019). Role of structural inheritance in the gravitational deformation of the Monviso meta-ophiolite Complex: the Pui-Orgiera serpentinite landslide (Varaita Valley, Western Alps). *Journal of Maps* 15(2), 372–381. DOI: https://doi.org/10.1080/17445647.2019.1602854

Gaidzik K., Żaba J., Ciesielczuk J. (2020) Tectonic control on slow-moving Andean landslides in the Colca Valley, Peru. *Journal of Mountain Sciences* 17: 1807–1825. DOI: http://dx.doi.org/10.1007/s11629-020-6099-y

Gee M. D. (1991) Classification of Landslide hazard zonation methods and a test of predictive capability landslides, In: Landslides-Glissements de Terrain, VI International Symposium on Landslides, Vol. 2, Christchurch, New Zealand, (1992), Balkema, Rotterdam, pp. 947–952. DOI: https://doi.org/10.4236/ojg.2016.63019

Ghazipour N. (2015) Study of the size and distribution of landslides in the Zagros Mountains (Iran). Ph.D. thesis. University of Geneva, Switzerland, 252p. DOI: http://dx.doi.org/10.1130/2016.2525(13)

Ghobadi M. H., Nouri M., Saedi B., Jalali S. H., Pirouzinajad N. (2017) The performance evaluation of information value, density area, LNRF, and frequency ratio methods for landslide zonationat Miandarband area, Kermanshah Province, Iran. *Arabian Journal of Geosciences* 10(19): 430. DOI: https://doi.org/10.1007/s12517-017-3202-y

Gibson I. L., Milliken K. L., Morgan J. K. (1996) Serpentinite-breccia landslide deposits generated during crustal extension at the Iberia Margin. In PROCEEDINGS-OCEAN DRILLING PROGRAM SCIENTIFIC RESULTS (pp. 571-576). NATIONAL SCIENCE FOUNDATION.

Guo C., Montgomery D. R., Zhang Y., Wang K., Yang Z. (2015) Quantitative assessment of landslide susceptibility along the Xianshuihe fault zone, Tibetan Plateau, China. *Geomorphology* 248: 93–110. DOI: http://dx.doi.org/10.1016/j.geomorph.2015.07.012

Gupta R. P., Joshi B. C. (1990) Landslide hazard zoning using the GIS approach—a case study from the Ramganga catchment, Himalayas. *Engineering geology* 28(1-2): 119–131. DOI: https://doi.org/10.1016/0013-7952(90)90037-2

Guzzetti F., Ardizzone F., Cardinali M., Galli M., Reichenbach P. (2008a) Distribution of landslides in the Upper Tiber River basin, central Italy. *Geomorphology* 96: 105–122. DOI: http://dx.doi.org/10.1016/j.geomorph.2007.07.015

Hajmolla Ali E. M., Tahooneh M., Shokri S. (2005) Geological Map of Silvana, Scale: 1:100.000, Sheet 4964. Geological survey and Mineral Exploration of Iran.

Hamza T., Raghuvanshi T. K. (2017) GIS based landslide hazard evaluation and zonation–A case from Jeldu District, Central Ethiopia. *Journal of King Saud University-Science* 29(2): 151-165. DOI: https://doi.org/10.1016/j.jksus.2016.05.002

Harrison J. V., Falcon N. L. (1937) The Saidmarreh landslip, Southwest Iran. *The Geographical Journal* 89: 42–47. DOI: https://doi.org/10.2307/1786990

Huang R. Q., Fan X. M. (2013) The landslide story. *Nature Geoscience* 6(5): 325–326. DOI: http://dx.doi.org/10.1038/ngeo1806

Kahal A. Y., Abdelrahman K., Alfaifi H. J., Yahya M. M. A. (2021) Landslide hazard assessment of the Neom promising city, northwestern Saudi Arabia: An integrated approach. *Journal of King Saud University – Science* 33: 101279. DOI: http://dx.doi.org/10.1016/j.jksus.2020.101279

Kamp U., Growley B. J., Khattak G. A., Owen L. A. (2008) GIS-based landslide susceptibility mapping for the 2005 Kashmir earthquake region. *Geomorphology* 101: 631–642. DOI: https://doi.org/10.1016/j.geomorph.2008.03.003

Karaoğlu Ö., Gülmez F., Göçmengil G., Lustrino M., Di Giuseppe P., Manetti P., Savaşçın M. Y., Agostini S. (2020) Petrological evolution of Karlıova-Varto volcanism (Eastern Turkey): Magma genesis in a transtensional triple-junction tectonic setting. *Lithos* 364–65: 105524. DOI: https://doi.org/10.1016/j.lithos.2020.105524

Kojima S., Nagata H., Yamashiroya S., Iwamoto N., Ohtani T. (2015) Large deep-seated landslides controlled by geologic structures: Prehistoric andmodern examples in a Jurassic subduction–accretion complex on the Kii Peninsula, central Japan. *Engineering Geology* 186: 44–56. DOI: https://doi.org/10.1016/j.enggeo.2014.10.018

Lee S., Kyungduck M. (2001) Statistical analysis of landslide susceptibil-ity at Yonging, Korea. *Environmental Geology* 40: 1095–1113. DOI: http://dx.doi.org/10.1007/s002540100310

Leir M., Michell A., Ramsay S. (2004) Regional landslide hazard susceptibility mapping for pipelines in British Columbia. Geo-engineering for the society and its environment. In: 57th Canadian geotechnical conference and the 5th joint CGS-IAH conference, 1–9.

Liu X., Su P., Li Y., Xu R., Zhang J., Yang T., Guo X., Jiang N. (2021) Spatial Patterns and Scaling Distributions of Earthquake-Induced Landslides-A Case Study of Landslides in Watersheds along Dujiangyan–Wenchuan Highway. *Frontiers in Earth Science* 9: 659152. DOI: http://dx.doi.org/10.3389/feart.2021.659152

Koyi H. (1998) The shaping of salt diapirs. Journal of Structural Geology 20 (4): 321-338. DOI: https://doi.org/10.1016/S0191-8141(97)00092-8

Machay F., El Moussaoui S., El Talibi H. (2023) Insights into large landslide mechanisms in tectonically active Agadir, Morocco: The significance of lithological, geomorphological, and soil characteristics. *Scientific African* 22: e01901. DOI: https://doi.org/10.1016/j.sciaf.2023.e01901

Melosh B. L. (2019) Fault initiation in serpentinite. *Geochemistry, Geophysics, Geosystems* 20: 2626–2646. DOI: http://dx.doi.org/10.1029/2018GC008092

Mohajjel M., Rasoli A. (2014) Structural evidence for superposition of transtension on transpression in the Zagros collision zone: Main Recent Fault, Piranshahr area, NW Iran. *Journal of Structural Geology* 62: 65–79. DOI: https://doi.org/10.1016/j.jsg.2014.01.006

Monsef I., Monsef R., Mata J., Zhang Z., Pirouz M., Rezaeian M., Xiao W. (2018) Evidence for an early-MORB to fore-arc evolution within the Zagros suture zone: Constraints from zircon U-Pb geochronology and geochemistry of the Neyriz ophiolite (South Iran). *Gondwana Research* 62: 287–305. DOI: https://doi.org/10.1016/j.gr.2018.03.002

Morgan J. P. Ranero R. (2023) Roles of Serpentinization in Plate Tectonics and the Evolution of Earth's Mantle. Chapter 21 -In "Dynamics of Plate Tectonics and Mantle Convection" book by Joau, C. Duarte (ISBN: 978-0-323-85733-8). DOI: https://doi.org/10.1016/B978-0-323-85733-8.00011-1

Myronidis D., Papageorgiou C., Theophanous S. (2016) Landslide susceptibility mapping based on landslide history and analytic hierarchy process (AHP). *Natural Hazards* 81(1): 245–263. DOI: https://link.springer.com/article/10.1007/s11069-015-2075-1

Neumann E. R., Abu El-Rus M. A., Tiepolo M., Ottolini L., Vannucci R., Whitehouse M. (2015) Serpentinization and Deserpentinization Reactions in the Upper Mantle beneath Fuerteventura Revealed by Peridotite Xenoliths with Fibrous Orthopyroxene and Mottled Olivine. *Journal of Petrology* 56 (1): 3–31. DOI: https://doi.org/10.1093/petrology/egu069

Nicoletti P. G., Parise M. (2002) Seven landslide dams of old seismic origin in southeastern Sicily (Italy), *Geomorphology* 46: 203-222. DOI: https://doi.org/10.1016/S0169-555X(02)00074-0

Pacheco Quevedo R., Velastegui-Montoya A., Montalván-Burbano N. Morante-Carballo F., Korup O., Daleles Rennó C. (2023) Land use and land cover as a conditioning factor in landslide susceptibility: a literature review. *Landslides* 20: 967–982. DOI: https://doi.org/10.1007/s10346-022-02020-4

Parker R. N., Hancox G. T., Petley D. N., Massey C. I., Densmore A. L., Rosser N. J. (2015) Spatial distributions of earthquake-induced landslides and hillslope preconditioning in the northwest South Island, New Zealand. *Earth Surface Dynamics* 3: 501–525. DOI: https://doi.org/10.5194/esurf-3-501-2015

Pirouz M., Avouc J. P., Hassanzadeh J., Kirschvink J. L., Bahroudi A. (2017) Early Neogene foreland of the Zagros, implications for the initial closure of the Neo-Tethys and kinematics of crustal shortening. *Earth and Planetary Science Letters* 477: 168–182. DOI: https://doi.org/10.1016/j.epsl.2017.07.046

Preiner M., Xavier J. C., Sousa F. L., Zimorski V., Neubeck A., Lang S. Q., Greenwell H. C., Kleinermanns K., Tuysuz H., McCollom T., Holm N., Martin W. (2018) Serpentinization: Connecting Geochemistry, Ancient Metabolism and Industrial Hydrogenation. *Life* 8: 41. DOI: https://doi.org/10.3390/life8040041

Rahimzadeh B., Bahrami S., Mohajjel M., Mahmoudi H., Haj-Azizi F. (2019) Active strike-slip faulting in the Zagros Mountains: geological and geomorphological evidence of the pull-apart Zaribar Lake basin, Zagros, NW Iran. *Journal of Asian Earth Sciences* 174: 332–345. DOI: https://doi.org/10.1016/j.jseaes.2018.12.017

Rahimzadeh B., Mahmoudi S., Corfu F., Ahadnejad V., Von Quadt A. (2021) A unique period of bimodal volcanism at 130–110 Ma in the northern Sanandaj-Sirjan Zone: Evidence for an extensional setting. *Lithos* 392: 106155. DOI: https://doi.org/10.1016/j.lithos.2021.106155

Roering J. J., Mackey B. H., Handwerger A. L., Booth A. M., Schmidt D. A., Bennett G. L., Cerovski-Darriau C. (2015) Beyond the angle of repose: A review and synthesis of landslide processes in response to rapid uplift, Eel River, Northern California. *Geomorphology* 236: 109–131. DOI: https://doi.org/10.1016/j.geomorph.2015.02.013

Saccani E., Allahyari K., Rahimzadeh B. (2014) Petrology and geochemistry of mafic magmatic rocks from the Sarve-Abad ophiolites (Kurdistan region, Iran): Evidence for interaction between MORB-type asthenosphere and OIB-type components in the southern Neo-Tethys Ocean. *Tectonophysics* 621: 132–147. DOI: https://doi.org/10.1016/j.tecto.2014.02.011

Saccani E., Allahyari K., Beccaluva L., Bianchini G. (2013) Geochemistry and petrology of the Kermanshah ophiolites (Iran): Implication for the interaction between passive rifting, oceanic accretion, and OIB-type components in the Southern Neo-Tethys Ocean. *Gondwana Research* 24(1): 392–411. DOI: https://doi.org/10.1016/j.gr.2012.10.009

Shoaei Z. (2014) Mechanism of the giant Seimareh Landslide, Iran, and the longevity of its landslide dams. *Environmtal Earth Sciences* 72: 2411–2422. DOI: http://dx.doi.org/10.1007/s12665-014-3150-8

Shoaei Z., Ghayoumian J. (1998) The largest debris flow in the world, Seimareh Landslide, Western Iran. In: Sassa K (ed) Environmental forest science. Springer, Dordrecht 553–561. DOI: https://doi.org/10.1007/978-94-011-5324-9_57

Soltani S., Saboohi R., Yaghmaei L. (2012) Rainfall and rainy days trend in Iran. *Climate Change* 110 (1–2): 187–213. DOI: http://dx.doi.org/10.1007/s10584-011-0146-1

Stocklin J. (1968) Structural history and tectonics of Iran; a review, vol 52. American Association of Petroleum Geologists, Tulsa, 1229–1258. https://doi.org/10.1306/5D25C4A5-16C1-11D7-8645000102C1865D

Stocklin J. (1990) The colourd mélange of the Makran: a product of dipirism? The first symposium of diapirism, Bandaar Abbas, Iran, 381–399.

Talbot C. J. Jackson M. P. A. (1987) Internal Kinematics of Salt Diapirs. *AAPG Bulletin* 71(9): 1068- 1093. DOI: https://doi.org/10.1306/703C7DF9-1707-11D7-8645000102C1865D

Talebian M., Jackson J. (2002) Offset on the main recent fault of NW Iran and implications on the late Cenozoic tectonics of the Arabia-Eurasia collision zone. *Geophysical Journal International* 150: 422–439. DOI: https://doi.org/10.1046/j.1365-246X.2002.01711.x

Tchalenko J. S., Braud J. (1974) Seismicity and structure of the Zagros: the Main Recent Fault between 33° and 35°N. Philos. *Philosophical Transactions of the Royal Society of London* 277: 1–25. DOI: https://doi.org/10.1098/rsta.1974.0044

Tibaldi A., Ferrari L., Pasquarè G. (1995) Landslides triggered by earthquakes and their relations with faults and mountain slope geometry: an example from Ecuador. *Geomorphology* 11 (1995): 215-226. DOI: https://doi.org/10.1016/0169-555X(94)00060-5

Wang X., Zhang L., Wang S., Lari S. (2014) Regional landslide susceptibility zoning with considering the aggregation of landslide points and the weights of factors. *Landslides* 11(3): 399–409. DOI: http://dx.doi.org/10.1007/s10346-013-0392-6

Zhang G., Cai Y., Zheng Z., Zhen J., Liu Y., Huang K. (2016) Integration of the statistical index method and the analytic hierarchy process technique for the assessment of landslide susceptibility in Huizhou, China. *Catena* 142: 233–244. DOI: http://dx.doi.org/10.1016/j.catena.2016.03.028

Zhao B., Hu Kh., Yang Z. Liu Q. (2022) Geomorphic and tectonic controls of landslides induced by the 2022 Luding earthquake. *Journal of Mountain Science* 19: 3323–3345. DOI: http://dx.doi.org/10.1007/s11629-022-7732-8

Zhou Y., Shi Zh., Zhang Q., Jang B., Wu Ch. (2019) Damming process and characteristics of landslide-debris avalanches. *Soil Dynamics and Earthquake Engineering* 121: 252-261. DOI: https://doi.org/10.1016/j.soildyn.2019.03.014

https://www.irimo.ir